Solid State Communications 149 (2009) 2210–2214

Contents lists available at ScienceDirect

Solid State Communications

journal homepage: www.elsevier.com/locate/ssc

Influence of oxygen partial pressure on structural, transport and magnetic properties of Co doped TiO_2 films

Bakhtyar Ali [a], Abdul K. Rumaiz [b], Arif Ozbay [b], Edmund R. Nowak [b], S. Ismat Shah [a,b,*]

[a] Department of Materials Science and Engineering, University of Delaware, Newark DE, 19716, United States
[b] Department of Physics and Astronomy, University of Delaware, Newark DE, 19716, United States

ARTICLE INFO

Article history:
Received 10 July 2009
Received in revised form
18 August 2009
Accepted 10 September 2009
by E.V. Sampathkumaran
Available online 16 September 2009

PACS:
75.50.Pp
75.60.Ej
77.84.Dy

Keywords:
A. Magnetic semiconductor
B. Pulsed laser deposition
D. Bound magnetic polaron
D. Magnetization

ABSTRACT

Pulse laser deposited (PLD) thin films of Co doped TiO_2 on silicon and quartz substrates are investigated. A mixture (1:1) of argon and oxygen with various total pressures (6.6 mPa to 53 Pa) is used to vary the oxygen content in the samples. The crystal structure and transport/ magnetic properties of $Co_xTi_{1-x}O_{2-\delta}$ ($x = 0.01, 0.03, 0.06$) thin films are found to have strong dependence on oxygen stoichiometry. X-ray diffraction (XRD) data reveal mixed phase material containing both anatase and rutile. However, the stability of each phase depends on the amount of oxygen present in the chamber during the growth of the films. X-ray Photoelectron Spectroscopy (XPS) shows the incorporation of Co in TiO_2 and is in the 2+ oxidation state. There occurs an enhancement in electrical conductivity and magnetization due to the off stoichiometric oxygen. The resistivity data follow a simple thermal activation model, giving carriers' activation energies in the range of 20 to 140 meV. A bound magnetic polaron model is adopted to explain the observed magnetic behavior of the films.

1. Introduction

TiO_2 has been thoroughly studied because of its widespread applications [1,2]. Its high dielectric constant and refractive index make it a promising material for optical coatings and protective layers [3]. Moreover, as a wide bandgap magnetic semiconductor, its applications in spintronics make it attractive [4]. In magnetic semiconductors, the host material is lightly doped with magnetic impurity without forming a second phase. The presence of magnetic impurities results in spin polarization in the majority carrier band. This polarization is induced by exchange interaction among the magnetic dopant spins and the carriers [5].

Room temperature ferromagnetism (RTFM) in Co doped TiO_2 has been the focus of research in recent years since its discovery by Matsumoto et al. [6]. However, the origin of ferromagnetism (FM) in such materials is still not clearly understood [7]. One of the key questions regarding the nature of the FM manifested by the magnetic oxide semiconductors is whether it is intrinsic or due to the segregation of the magnetic impurities. On the subject of the intrinsic nature of the magnetism, the work of Shinde et al. [8] shows that the solubility limit of Co in TiO_2 can be increased upon post annealing of the sample or growing the material at elevated temperatures. Similarly, the Co K-shell near-edge and extended X-ray absorption fine structure investigations of the charged state and local structure of Co in the epitaxial Co doped TiO_2 films rule out the presence of metallic Co or in the form of oxides [9]. The work of Griffin et al. also shows that there is no clustering of the magnetic impurity (Co) [10]. These findings indicate that it is quite possible to have Co substituted for Ti in the TiO_2 matrix.

In magnetic oxide semiconductors, the possible mechanisms responsible for FM exchange could be: Zener's double exchange [11], RKKY interaction [12], super exchange [13,14], and the bound magnetic polaron model (BMP) [15]. In all these models, carrier density plays an important role in mediating the FM coupling among the magnetic ions. The carrier density, in turn, is influenced by the nature of the defects present in the materials, e.g. interstitial defects, cation vacancies and/or oxygen vacancies [16–18].

Oxygen vacancies have a significant effect on the magnetic and transport properties of undoped [19,20] and transition metal doped TiO_2 [15,21]. In addition, TiO_2 can be reduced easily when exposed to an oxygen deficient environment. Also, the requirement of charge neutrality for Co doped TiO_2 suggests that

* Corresponding author at: Department of Materials Science and Engineering, University of Delaware, Newark DE, 19716, United States. Tel.: +1 302 831 1618; fax: +1 302 831 4545.
E-mail address: Ismat@udel.edu (S. Ismat Shah).

0038-1098/$ – see front matter © 2009 Elsevier Ltd. All rights reserved.
doi:10.1016/j.ssc.2009.09.011

doping should lead this system to being reduced even if enough oxygen is present [22–24]. To elucidate on the role of oxygen vacancies in affecting the structural, transport and magnetic properties of TiO_2, we studied cobalt doped TiO_2 films. These films were synthesized in a PLD system under various pressures of argon and oxygen gases premixed in the ratio 1:1. In this paper, we report the evolution of magnetic and transport properties of these films. The electrical transport of the films is well described by a simple thermal activation model. We discuss the observed ferromagnetism in our samples in light of the bound magnetic polaron theory.

2. Experimental

The films studied in this work were prepared via pulsed laser deposition (PLD) by laser ablating three different Co–TiO_2targets with 1%, 3% and 6% cobalt (Co) concentrations. Individual targets of various Co concentrations for PLD were prepared by mixing the appropriate amounts (wt%) of Co (99.998% Alfa-Aesar) and TiO_2 powders followed by grinding, pelletizing (350 MPa) and firing at 700 °C in an inert atmosphere of argon gas for 72 h. The pellets were fired three times with grindings between each firing to ensure the incorporation of Co in TiO_2. Finally, the target materials were characterized via XPS and XRD.

The targets were then laser ablated for 90 min by using an excimer laser (248 nm) at 400 mJ energy, with a pulse repetition rate of 15 Hz on boron doped silicon substrates (for magnetic measurements) and quartz substrates (for resistivity measurements). The base pressure in the chamber was $\sim 1.3 \times 10^{-5}$ Pa. The film deposition was carried out in the presence of a mixture of oxygen and argon gases (1:1). In order to vary the oxygen stoichiometry in the samples, the total pressure of the premixed gases was varied from 6.6 mPa to 53 Pa while the ratio of the mixture gases was kept constant, that is, 1:1. The variation in total pressure resulted in the change of oxygen content in the chamber and hence in the films. During deposition the substrate temperature was kept constant at 700 ± 5 °C for all the films. The thickness of the films (1–1.5 μ) was determined by both the profilometer (DekTek) and cross-sectional images from the scanning electron microscopy (SEM). Structural characterization of the films was carried out by using X-ray diffraction (XRD) (Rigaku X-ray D-Max diffractometer with Cu $K_\alpha = 1.5404$ Å equipped with graphite crystal monochromator). X-ray photoelectron spectroscopy (XPS) was performed on samples grown at various pressures (6.6 mPa to 53 Pa) using a SSI-M-probe equipped with Al K_α monochromatic X-ray source and an energy resolution of ∼0.1 eV. The base pressure in the XPS chamber was $\sim 1.3 \times 10^{-9}$ Pa prior to the start of data collection. For charge neutralization, a 1 eV e-beam was used. The charge correction was done using the carbon 1s (C 1s) peak as the reference, for which the binding energy is ∼284.6 eV. Transport and magnetic data were collected using quantum design's physical properties measurement system (PPMS) and quantum design's superconducting quantum interface device (SQUID). Electrical resistivity as a function of temperature was measured from room temperature down to 5 K. The sample's resistivity was determined from either a conventional four-probe resistance measurement or using an electrometer, depending on the sample's resistance. The results reported in this article were reproduced several times.

3. Results and discussion

The XRD scans of Co doped TiO_2 ($x = 0.03$) target material as well as films are shown in Fig. 1. All the peaks are associated with anatase and/or rutile phases. The XRD pattern of the target material showed a predominantly rutile structure. However, the XRD patterns of the samples show that the ratio of the two phases

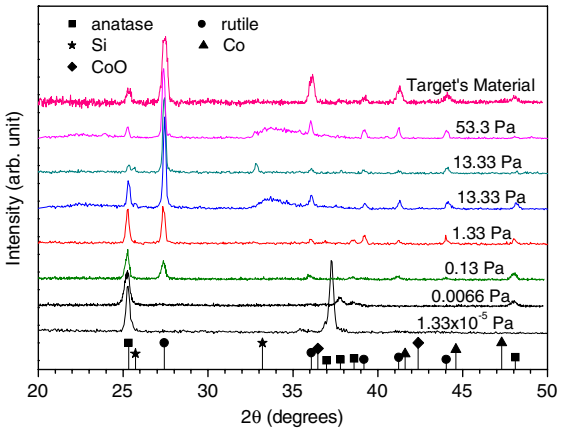

Fig. 1. XRD patterns of the target material and 3% Co doped TiO_2 films grown under various oxygen/argon (1:1) pressures.

(anatase and rutile) depend on the pressure of the gases ($Ar + O_2$) in the chamber during the synthesis. The only exception was the sample deposited under a vacuum with a base pressure 1.33×10^{-5} Pa and no added Ar or O_2. In this case, the material may have reduced to form some other type of Ti–oxide. Moreover, none of the samples show peaks corresponding to Co or CoO phases within the detection limit of XRD. It is important to note that for a given concentration of Co in TiO_2, changing the pressure resulted in the anatase–rutile transformation. A typical transformation for 3% Co doped sample is shown in Fig. 1, where at lower pressure, the anatase phase dominates. This anatase phase transforms to rutile with the increase of pressure. Finally, at higher pressure (53.33 Pa); the rutile phase becomes the dominant phase. The transformation process can be activated due to the formation of lattice defects [25]. These defects can be introduced in the material in different ways, including the addition of some non-isovalent dopants (particularly lower oxidation state than Ti^{4+}) which promote the anion vacancies for charge neutrality (Co^{2+} substitute Ti^{4+}) as well as cause lattice distortion [26]. Variation in the atmosphere (oxygen pressure) could be another reason for the phase transformation. All these parameters can destabilize the otherwise stable rutile system, promoting rutile–anatase phase transformation [27].

In order to check the presence of the metallic cobalt in these samples, high resolution XPS scans were performed. Fig. 2 shows the Co 2p region for the two films deposited under 6.6 mPa and 0.66 Pa pressures of the mixture gases (Ar and O_2). These spectra show four peaks: the $2p_{3/2}$ and $2p_{1/2}$ spin doublet and their corresponding shakeup resonant transition peaks at higher binding energy. The positions of Co $2p_{3/2}$ and Co $2p_{1/2}$ peaks are in agreement with those for Co in the formal oxidation state of 2+ in CoO [28,29]. If Co would have been present in the form of metallic clusters, the difference between Co $2p_{3/2}$ and $2p_{1/2}$ peaks would have been 15.05 [29], however, the separation between the $2p_{3/2}$ and $2p_{1/2}$ for our samples is measured to be 15.6 ± 0.1 eV which indicates that Co^{2+} is surrounded by oxygen in tetrahedral coordination. Moreover, the presence of the resonant shake up peaks along with the Co 2p doublets suggest that Co is in a high spin state [30,31]. This observation further confirms the substitution of Co on Ti sites. This trend was also observed in $Co_xTi_{1-x}O_2$ for $x = 0.01$ and 0.06 samples (data not shown). Thus within the detection limits of our XRD and XPS, the results obtained suggest that Co is predominantly incorporated in TiO_2.

In Fig. 3 the resistivity data of $Co_{0.03}Ti_{0.97}O_{2-\delta}$ films grown under various oxygen/argon pressures are shown. The resistivity as a function of temperature exhibits semiconducting behavior. Films grown under lower oxygen/argon pressures show small resistivity